Oncogene (2017) **36**, 5695–5708

www.nature.com/onc

ORIGINAL ARTICLE

ALDH1A3 is epigenetically regulated during melanocyte transformation and is a target for melanoma treatment

M Pérez-Alea[1], K McGrail[1], S Sánchez-Redondo[1,10], B Ferrer[1,2], G Fournet[3], J Cortés[4,5], E Muñoz[5], J Hernandez-Losa[2], S Tenbaum[6], G Martin[7], R Costello[8], I Ceylan[7], V Garcia-Patos[1,9] and JA Recio[1]

Despite the promising targeted and immune-based interventions in melanoma treatment, long-lasting responses are limited. Melanoma cells present an aberrant redox state that leads to the production of toxic aldehydes that must be converted into less reactive molecules. Targeting the detoxification machinery constitutes a novel therapeutic avenue for melanoma. Here, using 56 cell lines representing nine different tumor types, we demonstrate that melanoma cells exhibit a strong correlation between reactive oxygen species amounts and aldehyde dehydrogenase 1 (ALDH1) activity. We found that *ALDH1A3* is upregulated by epigenetic mechanisms in melanoma cells compared with normal melanocytes. Furthermore, it is highly expressed in a large percentage of human nevi and melanomas during melanocyte transformation, which is consistent with the data from the TCGA, CCLE and protein atlas databases. Melanoma treatment with the novel irreversible isoform-specific ALDH1 inhibitor [4-dimethylamino-4-methyl-pent-2-ynthioic acid-S methylester] di-methyl-ampal-thio-ester (DIMATE) or depletion of *ALDH1A1* and/or *ALDH1A3,* promoted the accumulation of apoptogenic aldehydes leading to apoptosis and tumor growth inhibition in immunocompetent, immunosuppressed and patient-derived xenograft mouse models. Interestingly, DIMATE also targeted the slow cycling label-retaining tumor cell population containing the tumorigenic and chemoresistant cells. Our findings suggest that aldehyde detoxification is relevant metabolic mechanism in melanoma cells, which can be used as a novel approach for melanoma treatment.

Oncogene (2017) **36,** 5695–5708; doi:10.1038/onc.2017.160; published online 5 June 2017

INTRODUCTION

Melanoma is the most lethal form of skin cancer with an increasing incidence and poor prognosis.[1] Melanoma heterogeneity and tumor resistance to therapy hamper effective treatment of melanoma. During the last few years, new drugs, such as BRAF inhibitors or immunomodulatory therapies, have been developed; however, long-lasting effects are minimal or are only effective in a minority of patients,[2–4] highlighting the need for new therapeutic alternatives.

Aldehyde dehydrogenases (ALDHs) enzymes have a key role in the detoxification metabolism of aldehydes, which have a broad spectrum of biological activities. ALDH activity is crucial to the biosynthesis of retinoic acid, betaine and carnitine, alcohol metabolism and cellular homeostasis.[5–7] They also can act as esterases[8] and perform non-enzymatic functions, such as the reduction of osmotic stress and protection from ultraviolet exposure.[9,10] ALDHs are found in all subcellular compartments, including the cytosol, endoplasmic reticulum, mitochondria and the nucleus, with some even found in more than one location.[11]

Recent evidence suggests that enhanced ALDH activity is a hallmark of cancer stem cells (CSC) measurable by the ALDEFLUOR assay, most likely due to multiple or distinct ALDH isozymes, the contribution of each depending on the specific type of tumor.[12] High ALDH activity has been demonstrated in tumorigenic cells from several tumor types, including myeloid leukemia,[13] mammary gland,[14] colon,[15,16] liver,[17] pancreas[18] and prostate.[19] Although the existence of these types of cells is controversial in melanoma, a role for ALDH1 in tumorigenesis and as a marker of melanoma CSCs has been suggested.[20,21] Moreover, other investigations have shown that ALDHs could be key determinants for the survival and drug resistance of cancer cells.[22]

The current development of ALDH inhibitors is being driven by emerging clinical needs. However, pharmacological inhibitors have been developed for only 3 of the 19 ALDH isozymes.[23] These are the enzymes involved in the metabolism of alcohol (ALDH2) and the anticancer oxazaphosphorine drugs (ALDH1A1 and ALDH3A1).[24] Among the molecules known to inhibit ALDH activity, there are reversible inhibitors, competitive substrates or molecules whose metabolic products mediate the ALDH activity.[24] Within these latter type of molecules, disulfiram, which inhibits ALDH1A1 and ALDH2, is being evaluated in clinical trials; however, it also inhibits carboxylesterase and cholinesterase and causes a variety of physiological side effects.[24] Furthermore, its efficacy as an anticancer agent is still

[1]Biomedical Research in Melanoma-Animal Models and Cancer Laboratory-Oncology Program, Vall d´Hebron Research institute VHIR-Vall d'Hebron Hospital, Barcelona-UAB, Spain; [2]Anatomy Pathology Department, Vall d'Hebron Hospital, Barcelona-UAB, Spain; [3]Institut de Chimie et Biochimie Moléculaire et Supramoléculaire, UMR-CNRS 5246, Université de Lyon, Université Claude Bernard-Lyon1, Villeurbanne, France; [4]Ramon y Cajal University Hospital, Madrid, Spain; [5]Clinical Oncology Program, Vall d'Hebron Institute of Oncology-VHIO, Vall d'Hebron Hospital, Barcelona-UAB, Spain; [6]Stem Cells and Cancer Laboratory, Vall d'Hebron Institute of Oncology, Barcelona, Spain; [7]Advanced BioDesign, Parc Technologique de Lyon, Woodstock - Bâtiment Cèdre 1, Saint Priest, France; [8]Service d'Hématologie et Thérapie Cellulaire, Centre Hospitalier Universitaire La Conception, Marseille, France and [9]Dermatology Department, Vall d'Hebron Hospital, Barcelona-UAB, Spain. Correspondence: Dr JA Recio, Biomedical Reseach in Melanoma-Animal Models and Cancer Laboratory, Institut de Recerca Vall d'Hebron-VHIR, Lab 203 Ed. Collserola, 119-129 Passeig Vall d'Hebron, Barcelona 08035, Spain.
E-mail: juan.recio@vhir.org
[10]Current address: Microenvironment and Metastasis Group at CNIO, Madrid 28029, Spain.
Received 18 October 2016; revised 18 April 2017; accepted 18 April 2017; published online 5 June 2017

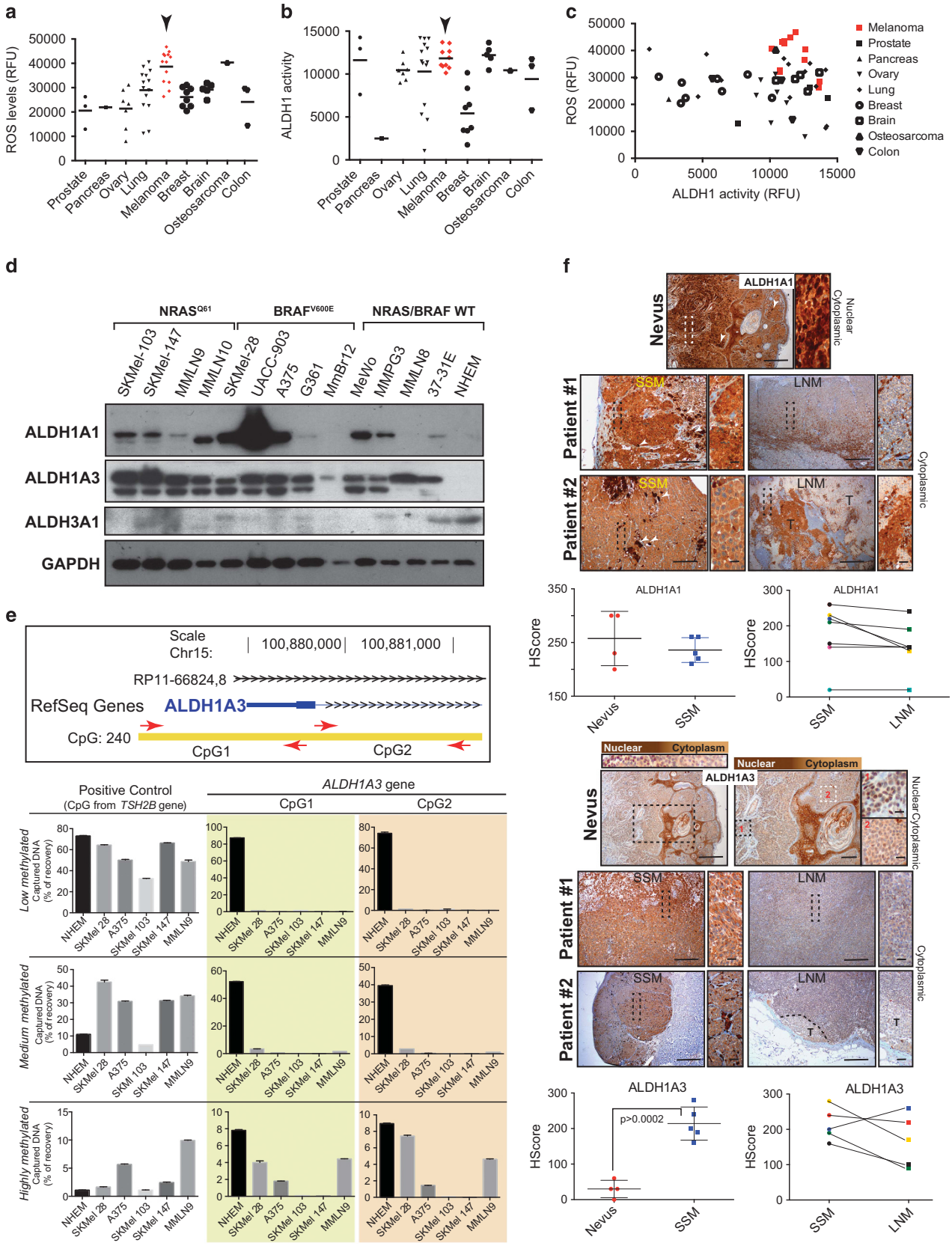

not established as it does not inhibit the growth of mouse lymphoid cells overexpressing the *Bcl2* gene.[25]

Di-methyl-ampal-thio-ester (DIMATE) is a novel competitive irreversible inhibitor of ALDH1 and ALDH3.[26] Although it inhibits cancer cell growth irreversibly, this effect was reversible on normal human prostate epithelial cells.[27] Moreover, intraperitoneal injection of DIMATE in an animal model appeared to be effective in the prevention or treatment of peritoneal carcinomatosis.[28] Melanoma tumors produce a high amount of reactive oxygen species (ROS) as a result of an increased metabolism of transformed cells, immune reaction against the developing tumor, ultraviolet radiation, melanin production and an altered antioxidant system.[29] Among the many actions of ROS in biological systems, the peroxidation of unsaturated lipids is well established[30] and is of particular importance because it gives rise to toxic aldehydes that are highly apoptogenic. Indeed, one such toxic aldehyde malondialdehyde (MDA) is a chromatin cross-linking agent.[31] Another is 4-hydroxynonenal (HNE) that induces apoptosis and whose apoptogenecity is inhibited when cells are transfected by the ALDH3 gene.[32] For cells to survive, these apoptogenic aldehydes must be metabolized and converted into less reactive non-apoptogenic molecules. The oxidation of aldehydes in general has been abundantly documented in the literature for over 30 years. More recently, the oxidation of specific aldehydes has been ascribed to particular ALDH isoforms.[33] Hence, targeting ALDHs could provide a novel avenue for treatment, especially for melanoma, by increasing the accumulation of pro-apoptotic molecules. Here, we show that the *ALDH1A3* isoform is epigenetically deregulated during melanocyte transformation, switching its localization during establishment and correlating with the production of high amounts of ROS. Treatment of patient-derived tumors with DIMATE reduced tumor growth by increasing apoptosis in cycling tumor cells and in a slow cycling label-retaining cell sub-population.

RESULTS

The high amount of ROS in melanoma cells correlates with an elevated ALDH1 activity

There is evidence for the presence of an aberrant redox state in melanoma. Melanoma tumor cells have higher levels of superoxide anion (O_2^-) and aberrant activation of transcription pathways related to oxidative stress.[34] In this context, initially, we confirmed this observation by measuring the amount of ROS in 13 different melanoma cell lines, including five patient-derived cell lines, among other tumor cell types (a total of 56 cell lines from nine different tumor types, Supplementary Figure S1A). Melanoma cells showed the highest amounts of ROS compared with most of the other tumor cell types (Figure 1a). ALDH isoforms have an important role in a wide variety of metabolic processes.[35,36] Interestingly, melanoma cells had a consistently elevated activity of ALDH1 (Figure 1b) and showed the strongest correlation between the amount of ROS and the ALDH1 activity, among the other tumor cell types investigated (Figure 1c). Moreover, melanoma cells showed an inverse correlation between the amount of ROS and the ALDH1 activity (Figure 1c). Thus, these results suggest an important role of ALDHs in melanoma homeostasis.

ALDH1A3 is highly expressed in melanomagenesis and progression

To date, 19 ALDH genes have been identified in the human genome.[11] ALDH1 activity has been related to normal stem cells (SCs) and CSCs.[37] Although the increased activity of ALDH1 has been correlated with poor prognosis in a number of tumor types, melanoma appears to be an exception.[38,39] Analysis of ALDH isoform expression using the cancer cell line encyclopedia database (CCLE) (http://www.broadinstitute.org/ccle) showed that *ALDH1A3* is the isoform most abundantly expressed in melanoma, whereas *ALDH1A1* was moderately expressed and *ALDH3A1* was almost absent (Supplementary Figure S1B). Similar results were obtained when the mRNA expression data were analyzed from the TCGA database (TCGA; cBioportal; http://www.cbioportal.org) (Supplementary Figure S2). Consistent with this finding, our set of melanoma cells expressed ALDH1A3 and not ALDH3A1, and protein expression of isoform ALDH1A1 was variable among the cell lines tested (Figure 1d). In contrast, normal human epidermal melanocytes did not express ALDH1A3 and showed elevated amounts of ALDH3A1 protein (Figure 1d). The switch in the isoform protein expression observed in melanoma cells compared with normal melanocytes was confirmed at the mRNA level. *ALDH1A3* mRNA was highly expressed in all melanoma cell lines, whereas *ALDH3A1* expression was mostly repressed and *ALDH1A1* mRNA amounts were variable (Supplementary Figures S3A and B). The marked change in *ALDH1A3* mRNA and protein expression observed in melanoma cells compared with melanocytes suggested an epigenetic regulation of the gene. Analysis of a CpG island located at the *ALDH1A3* gene 5'-end regulatory sequence showed that this region was highly methylated in normal melanocytes, whereas melanoma cells lacked this modification (Figure 1e and Supplementary Figure S3C). According to the human protein atlas database (http://www.proteinatlas.org), ALDH1A1 and ALDH1A3 were overexpressed in 25 and 60% of the melanoma samples, respectively, ALDH3A1 was not expressed and none of the isoforms were detected in normal tissue. These results were also observed in our set of melanoma samples (Supplementary Figures S3D and E). ALDH protein expression analysis during melanoma progression (nevus, primary melanoma and lymph node metastasis from the same patient) showed that ALDH1A1 was present in the nucleus and cytoplasm of benign lesions and was only detected in the cytoplasm of primary tumors without significant changes in the amount of protein during progression. In four out of five paired primary tumors and lymph node metastases, the amount of ALDH1A1 tended to diminish in the metastases (Figure 1f). Notably, ALDH1A3 appeared to be nuclear in the most differentiated cells of the nevus, switching its

Figure 1. Melanoma cells have elevated amounts of ROS, ALDH1 activity and express high amounts of ALDH1A3. (**a**) Amount of ROS in 56 different cell lines representing 9 different tumor types. The amount of ROS observed in each cell line and the mean ROS in each type of tumor are shown (relative fluorescence units (RFUs)). (**b**) Graph shows the different amounts of ALDH1 activity in each cell line and the mean ALDH1 activity in each tumor type. (**c**) Correlation between the amount of ALDH1 activity and ROS among different tumor cell types. Markers for melanoma cells are in red. (**d**) Western blot showing the amounts of ALDH1A1, ALDH1A3 and ALDH3A1 in the different melanoma cell lines. GAPDH is the loading control. (**e**) DNA methylation analysis of a CpG island located in the ALDH1A3 regulatory promoter region. Two sets of primers covering the region (240 bp) were designed (CpG1 and CpG2). Analysis was performed in normal human epidermal melanocytes (NHEM), $BRAF^{V600E}$ mutant cells (SKMel-28, A375) and $NRAS^{Q61}$ mutant cells (SKMel-103, SKMel-147 and patient-derived MMLN9). (**f**) Immunohistochemistry of ALDH1A1 and ALDH1A3 in human samples. Expression of the different isoforms and subcellular localization are shown in a nevus, superficial spreading melanoma (SSM) and lymph node metastasis (LNM), the latter two from the same patient. HScores from ALDH1A1 and ALDH1A3 staining performed in nevi and SSM and HScores for the ALDH1A1 and ALDH1A3 staining of the paired SSM and LNM samples from same patients are shown below. Arrows indicate melanophages. Bars represent 500 and 50 μm for the magnifications. *P*-value was calculated by Student´s *t*-test.

localization to the cytoplasm as cells become more undifferentiated and grouped in typical nests. Primary melanomas showed a significant increase in the cytoplasmic expression of ALDH1A3 compared with benign lesions that tended to decrease in the paired lymph node metastasis (Figure 1f). Altogether, these results indicate that ALDH isoforms are subjected to expression regulation during melanocyte malignancy, whereas ALDH1A3 expression and its subcellular localization are biomarkers for melanomagenesis and melanoma progression, respectively.

Inhibition of ALDH1 by DIMATE is cytotoxic for melanoma

Several studies have confirmed that increased ALDH activity is a surrogate marker for human and murine cells with increased proliferation and tumorigenic potential.[40] The above results posit melanoma as a candidate tumor for targeting the ALDH1 isoform. DIMATE is an alpha, beta-acetylenic aminothiol ester, with specific inhibitory activity against ALDH1 and ALDH3 isoforms.[26,27] We determined the IC_{50} of DIMATE for all of the melanoma cell lines, including five patient-derived cell lines and a mouse melanoma cell line. The results showed that the IC_{50} of DIMATE for melanoma cells ranged between 3 and 15 μM, whereas the proliferation and survival of normal melanocytes was not affected by this compound (Figure 2a, Supplementary Table S1). Conventional drugs, including dacarbazine, showed a lower efficacy toward patient-derived cells (Supplementary Figure S4A). Melanoma was among the tumor types more sensitive to DIMATE treatment (Figure 2b, Supplementary Table S1). Furthermore, there was a positive correlation between ALDH1 activity and the IC_{50} for DIMATE and a negative correlation between the sensitivity of cells to DIMATE and the ROS amount (Figures 2c and d), which is in agreement with the inverse correlation between the amount of ROS and the ALDH1 activity showed by these cells (Figure 1c). Consequently, the sensitivity of cells to DIMATE diminished by the addition of glutathione-monoethyl-ester or the ROS scavenger *N*-acetyl-cysteine (Supplementary Figures S4B and C). However, we did not observe significant differences in the IC_{50}, ALDH1 activity or the amount of ROS between the cells harboring *BRAF* or *NRAS* mutations (despite the low number of cell lines included in each group) (Figure 2e). Thus, these results indicate that DIMATE is effective against melanoma proliferation and survival.

DIMATE promotes the accumulation of HNE and MDA leading to apoptosis

One of the consequences of the elevated amounts of ROS in melanoma cells is the generation of apoptogenic aldehydes such as MDA and HNE. Tumor cells protect themselves from the apoptogenic effect of these aldehydes by the ALDHs that oxidize them to their non-apoptogenic carboxylic acids.[41] Treatment of mouse and human melanoma cells harboring different genetic backgrounds with DIMATE increased the amount of HNE adducts in proteins, as early as 6 h after treatment (Figure 2f). DIMATE caused apoptosis in a time course-dependent manner in all of the cell lines tested (Figure 2g). The apoptotic response was also observed at the molecular level with the increase of BAX and the disappearance of BclX (Figure 2h).

DIMATE inhibits melanoma tumor growth with low toxicity

Next, we analyzed DIMATE efficacy as an inhibitor of *in vivo* tumor growth. To this end, we used three different mouse models including an immunocompetent mouse model and four different melanoma cell lines comprising a mouse melanoma cell line, two established human melanoma cell lines (harboring $BRAF^{V600E}$ or $NRAS^{Q61L}$ mutations) and patient-derived melanoma cells. The immunocompetent mouse model showed that the maximum effect of DIMATE was achieved at a 14 mg/kg regimen administered 3 days per week. Administration of the drug daily did not increase tumor efficacy (Figure 3a), and according to weight measurements and the blood parameters, we detected liver toxicity only at 28 and 42 mg/kg under a daily treatment (7 days per week) regimen (Figure 3a and Supplementary Table S2). These data were also consistent with the bio-distribution of the drug in rats where DIMATE could be still detected in the kidneys and liver 5 days after a single dose (20 mg/kg) while it was below detection levels in the skin at 48 h post treatment (Supplementary Figure S4D). Independent of the dose and treatment regimen, all of the treated tumors showed indications of the efficacy of DIMATE as an ALDH inhibitor with positive staining for HNE and MDA and as an apoptogenic compound with cleaved caspase-3 and extensive areas of necrosis (Figure 3b and Supplementary Figure 5A). The molecular analysis of tumor samples correlated with the pro-apoptotic effect of the aldehydes (Figure 3c). Analysis of melanoma relevant pathways in tumor samples by immunohistochemistry did not reveal significant differences in the activation of RAS or phosphatidylinositol 3 kinase pathways according to the surrogate markers p-ERK1/2 and p-S6, respectively. However, although samples were positive for the proliferation marker Ki67, they were mostly negative for cyclin D1 (Supplementary Figure S5B).

We investigated the *in vivo* drug efficacy using a $BRAF^{V600E}$ mutated cell line (SKMel-28) and cell line harboring an $NRAS^{Q61L}$ mutation (SKMel-103). DIMATE reduced tumor growth by approximately 60–70% in both cases after 2 weeks of treatment (Figures 4a and b). We next investigated DIMATE activity against patient-derived cells. Treatment of cells with DIMATE *in vitro* for 48 h led to the accumulation of HNE bound to proteins and apoptosis (Figure 4c). DIMATE significantly reduced patient-derived xenograft growth between 50 and 60% despite the higher complexity of these cells expressing multiple ALDH isoforms (Supplementary Figure S3B). Tumor growth reduction was associated with the accumulation of toxic aldehydes bound to proteins and apoptosis (Figure 4d).

DIMATE targets slow cycling label-retaining melanoma tumor cells

Tumor recurrence after chemotherapy is a major cause of patient morbidity and mortality. Slow cycling, label-retaining tumor cells exhibit a multifold increase in their ability to survive traditional forms of chemotherapy and reenter the cell cycle.[42,43] To study whether DIMATE targets slow cycling cells, we infected patient-derived cells with an inducible expression vector containing a histone 2B–green fluorescent protein (GFP) (H2B–GFP) fusion protein. Induction of the expression of H2B-GFP by the addition of doxycycline for 3 days led to the labeling of 82% of the cell population. After withdrawal of doxycycline, dividing cells lost half of the dose with each cell division. Seven days after withdrawal, only 3.4% of cells retained the marker (Supplementary Figure S6A). We studied whether DIMATE targeted this slow cycling population *in vitro* and *in vivo*. The slow cycling label-retaining cell population was diminished upon DIMATE treatment *in vitro* (from 2.8% untreated to 0.001% treated) (Figure 5a). To test this *in vivo*, we induced the expression of H2B-GFP in patient-derived cells. Induction (doxycycline treatment) was sustained until the tumors reached a volume of 50–100 mm^3. Then, the mice were distributed into different groups of treatment in the absence of doxycycline. At the end point of the experiment, human GFP-positive cells (slow cycling cells) were isolated and quantified (Figure 5b and Supplementary Figure S6B). We observed a significant reduction the slow cycling cell population in DIMATE-treated mice in a dose dependent manner (approximately 12%—untreated; 4%—7 mg/kg; 0.8%—14 mg/kg) (Figure 5b). Thus, DIMATE is not only effective in reducing bulk tumor growth but in addition, it targets the slow cycling label-retaining tumor cell population.

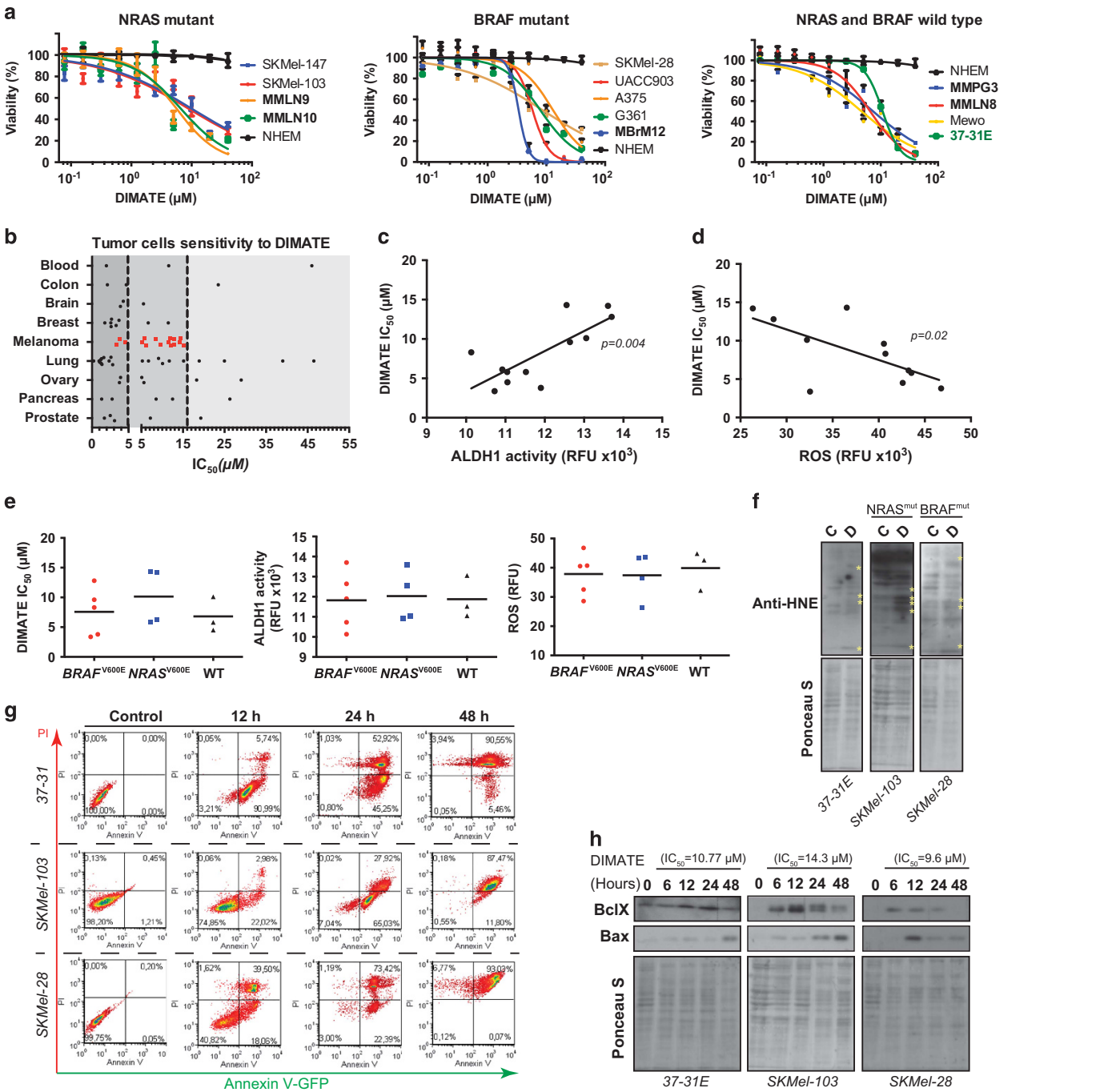

Figure 2. DIMATE reduces melanoma cells viability, promoting HNE-protein adducts leading to apoptosis. (**a**) Viability assay of melanoma cells exposed to increasing concentrations of DIMATE. Cells were grouped according to their NRAS and BRAF mutational status. In names in bold represent patient-derived cell lines, in green mouse melanoma cell line, NHEM represent normal human epidermal melanocytes. All of the experiments were performed in triplicate ($n = 3$). (**b**) Graph showing the IC_{50} concentrations in different tumor cell lines. Each dot corresponds to a cell line. Red dots represent melanoma cell lines. Dark gray = very sensitive, medium gray = sensitive, light gray = resistant. (**c**) Graph showing correlation between ALDH1 activity (GFSEF12 1.6 μM, RFU, relative fluorescence unit) and the IC_{50} for DIMATE in melanoma cell lines (Correlation Pearson r (two tailed)). (**d**) Graph showing correlation between ROS (RFUs) abundance and the IC_{50} for DIMATE in melanoma cell lines (Correlation Pearson r (two tailed)). Values for all cell lines are shown in Supplementary Table S2. (**e**) Graphs showing the DIMATE IC_{50}, ALDH1A1 activity and ROS amount according to the mutational status of the cell lines. Horizontal bars show the mean value. (**f**) DIMATE treatment promotes the accumulation of HNE adducts and apoptosis. Western blot showing the accumulation of HNE-protein adducts. Cell lines were either untreated (C) or treated with DIMATE (D) at their IC_{50} concentrations for 6 h. Asterisks mark the bands with an increased accumulation of HNE adducts. Ponceau S staining of the membrane is shown for loading control. A representative experiment is presented ($n = 3$). (**g**) DIMATE treatment induces apoptosis. The same cell lines as in **f** were treated with DIMATE for 48 h ([DIMATE] = IC_{50} for each cell line). Cells were collected at the different time points indicated. A representative experiment is presented ($n = 3$). (**h**) Western blot showing the amounts of BclX and BAX in protein extracts from the cells treated as in **g**. Membrane staining with Ponceau S is shown as a loading control. Experiments were repeated at least three times. PI, propidium iodide.

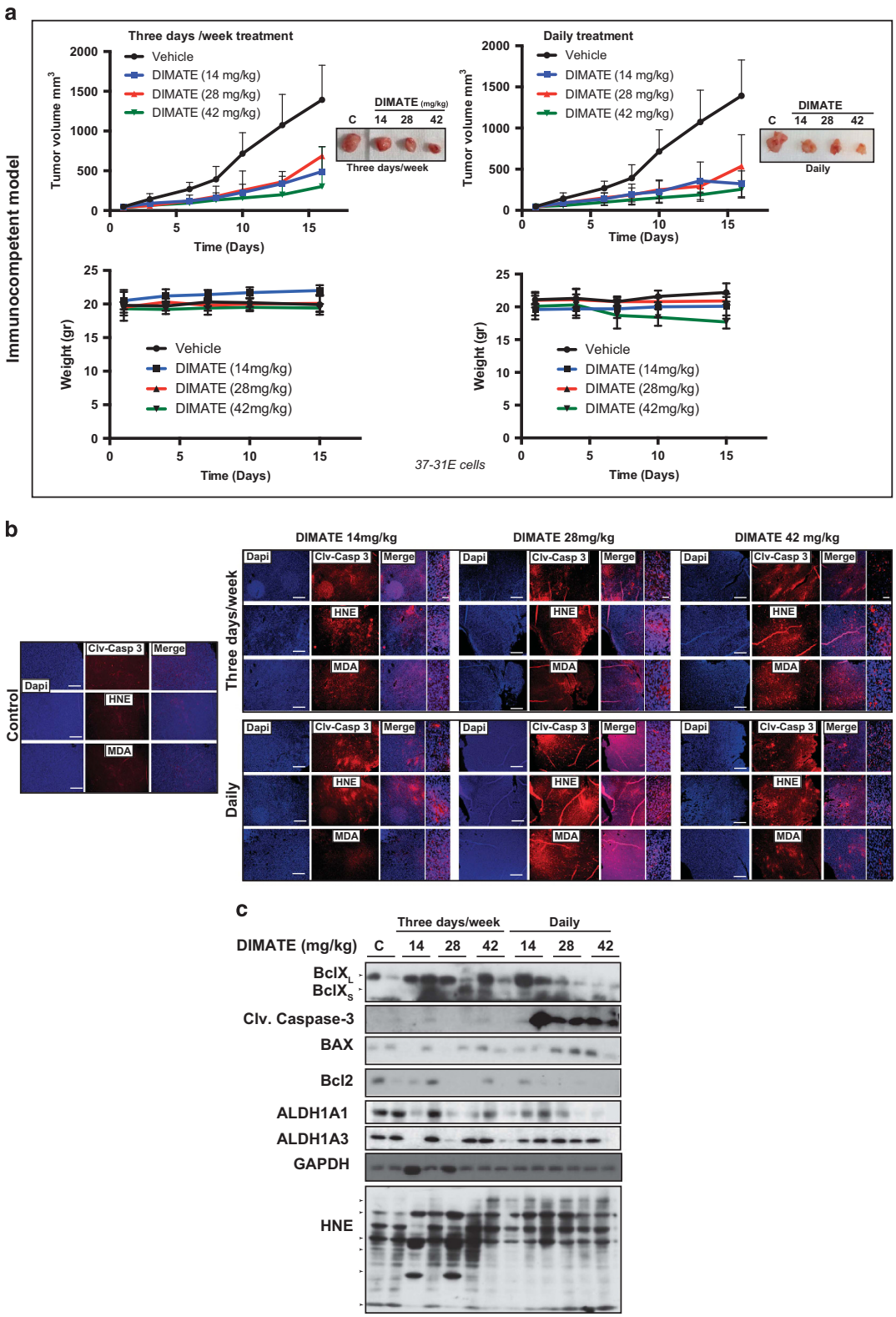

Figure 3. DIMATE treatment reduces *in vivo* tumor growth in an immunocompetent model by inducing apoptosis. (**a**) *In vivo* tumor growth curves in an immunocompetent mouse model ($n = 5$ mice per group of treatment) using 37-31E cells. Two different regimens of treatment (3 days per week or daily) and three different doses (14, 28 or 42 mg/kg) were used. A representative image of the tumor size in each condition is shown. (**b**) DIMATE treatment causes the accumulation of HNE and MDA and apoptosis. Representative immunofluorescence images of tumors from different treatment groups stained against HNE, MDA or cleaved caspase-3. Bars represent 500 and 50 μm in the magnifications. (**c**) Western blot showing the expression of the apoptotic markers BclX, cleaved caspase-3 and BAX in tumor samples. GAPDH is shown as a loading control, and anti-HNE is used to demonstrate the accumulation of these protein adducts after DIMATE treatment. Two different tumors are shown per condition.

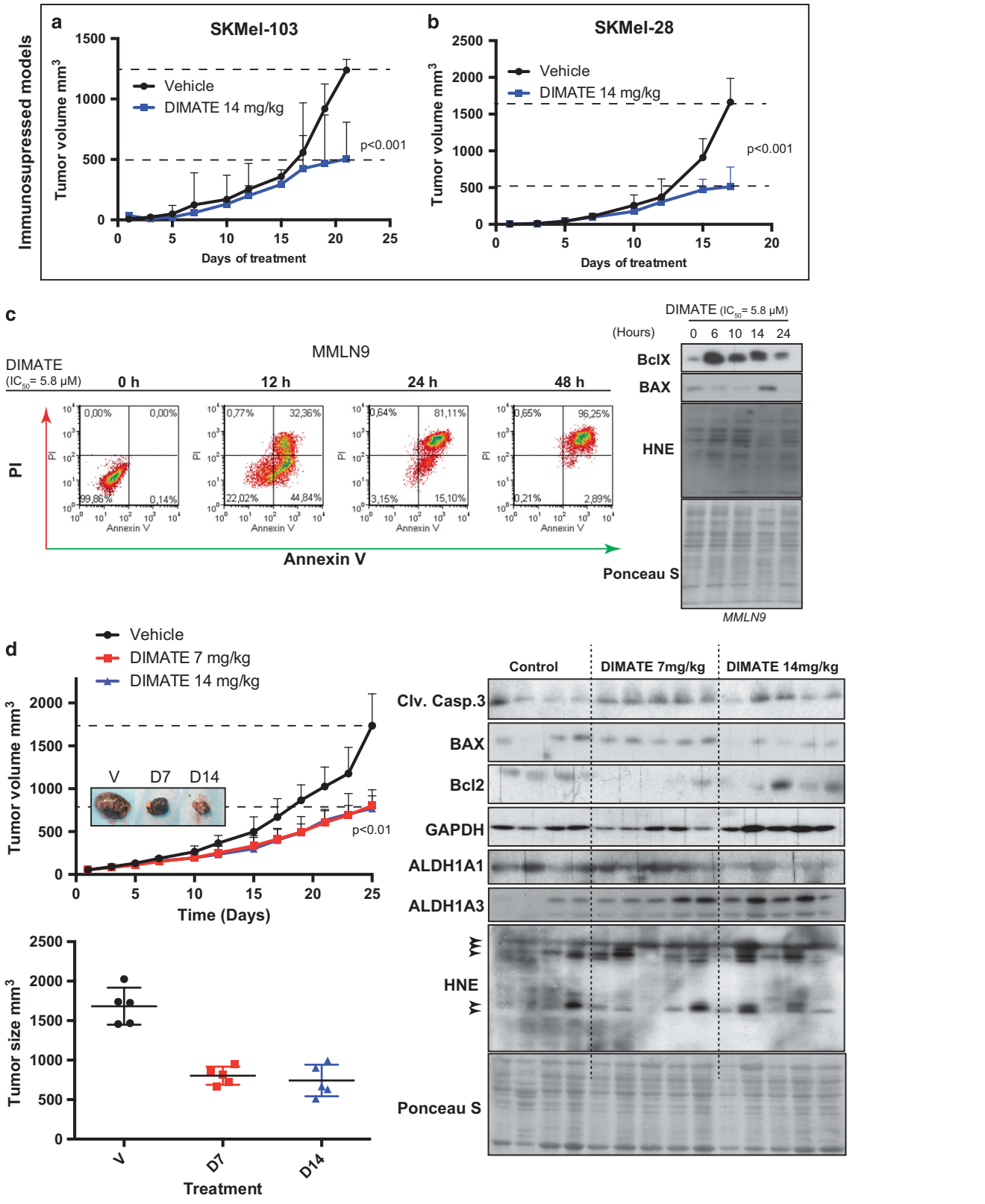

Figure 4. DIMATE *in vivo* efficacy is genotype independent and is also efficient against patient-derived xenografts. (**a**) *In vivo* tumor growth of *NRAS* mutant SKMel-103 cells ($n = 5$ mice per group). (**b**) *In vivo* tumor growth of *BRAF* mutant cells SKMel-28 ($n = 5$ mice per group). (**c**) MMLN9 patient-derived cells treated with DIMATE. Apoptosis was measured by flow cytometry at different time points of treatment. (PI: propidium iodide, Annexin V: GFP-annexin V). Western blot shows molecular markers of apoptosis upon DIMATE treatment. Ponceau S staining is shown as a loading control. (**d**) *In vivo* tumor growth curves of MMLN9 patient-derived cells ($n = 5$ mice per group) treated with two different doses of DIMATE. *P*-value was calculated by Student´s *t*-test. Graph below shows the tumor size within each group ($n = 5$ mice per group). Western blot shows the apoptosis molecular markers within the tumors. Ponceau S staining and GAPDH are shown as loading controls.

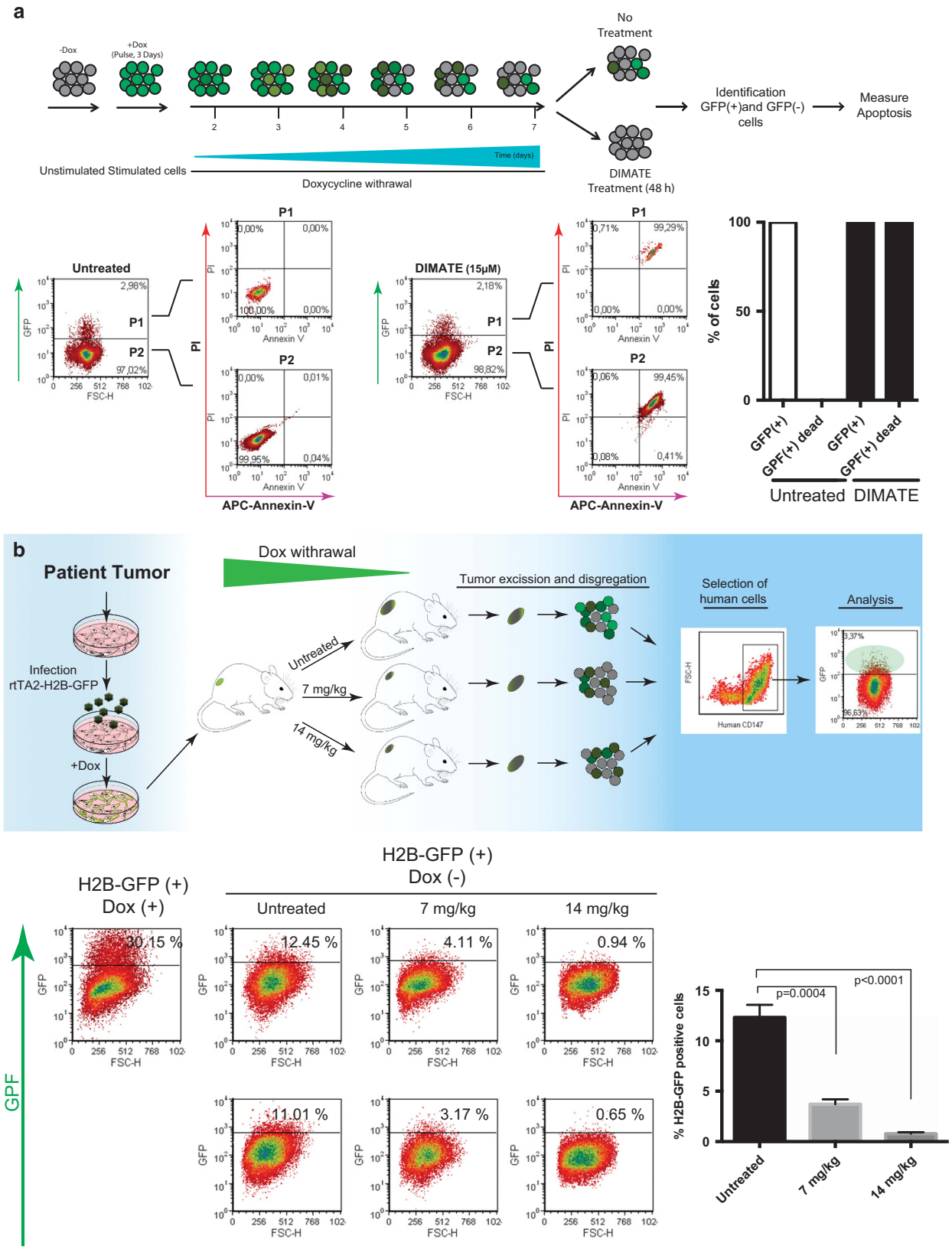

Figure 5. DIMATE targets patient-derived slow cycling cells *in vitro* and *in vivo*. (**a**) MMLN9-H2B-GFP cells were treated with doxycycline for 5 days. Then, doxycycline was withdrawn for 9 days and the cells were treated with DIMATE (15 μM). The number of GFP-positive cells was analyzed by flow cytometry. A representative experiment out of three is shown. (**b**) Scheme for the *in vivo* procedure to evaluate DIMATE´s efficacy in targeting slow cycling patient-derived cells. Below, flow cytometry analysis of human cells isolated from xenograft tumors under the different treatment conditions. Two tumors per condition are shown. The graph shows the percentage of slow cycling cells isolated in each group ($n = 4$ tumors). *P*-value was calculated by Student's *t*-test. APC, allophycocyanin; PI, propidium iodide.

Targeting *ALDH1A1* and *ALDH1A3* by short hairpin RNA (shRNA) mimics the effect of DIMATE inhibiting cell proliferation, survival and *in vivo* tumor growth

Next, we genetically validated DIMATE's targets (ALDH1A1 and ALDH1A3) by generating three melanoma cell lines ($BRAF^{V600E}$ mutant SKMel-28, $NRAS^{Q61L}$ SKMel-103 and patient-derived cell $NRAS^{Q61K}$ mutated MMLN9) infected with an inducible system expressing either a scrambled-shRNA, *ALDH1A1*-shRNA or *ALDH1A3*-shRNA (Supplementary Figure S7A). Knockdown of either *ALDH1A1* or *ALDH1A3* significantly decreased cell proliferation in three-dimensional growth assays in all of the cell lines without variations in the number of colonies formed. However, simultaneous knockdown of both isoforms significantly reduced the number of colonies and cells (Figure 6a and Supplementary Figure S7B). Similar results were observed when we tested the melanospheres formation capability. Depletion of *ALDH1A3* or *ALDH1A1* and *ALDH1A3* significantly reduced the number of melanospheres in the three different cell lines tested (Figure 6b and Supplementary Figure S7C). The above results were validated in the three cell lines using three different small interfering RNA sequences for each gene (Supplementary Figure S8), and correlated with a significant increase in apoptotic cells at 9 and 12 days after shRNA induction (Figure 6c). Furthermore, *in vivo* tumor growth experiments using SKMel-103 cells showed that knocking down either *ALDH1A1* or *ALDH1A3* reduced tumor growth and silencing both isoforms impeded tumor development (Figure 6d). These data are also consistent with the mechanism of action of DIMATE, suggesting that inhibition of ALDH1A1, ALDH1A3, or both compromises cell proliferation and survival.

DISCUSSION

Melanomas possess many types of oxidative species that are important mediators of tumor transformation and progression of the disease. To protect themselves from these anomalies, tumor cells have developed antioxidant measures and enzymatic adjustments necessary to avoid toxic accumulation and promote their survival. These detoxification enzymes provide valuable targets for melanoma treatment. Here, we have shown that melanomas induce the expression of a specific detoxification enzyme (ALDH1A3). This enzyme, among other functions, helps to manage the indirect harmful effects of ROS, such as the production of toxic aldehydes, and reveals a new feature that can be exploited therapeutically. Specifically, our results show the efficacy of the novel molecule DIMATE as an inhibitor of ALDH1 activity that on one hand leads to tumor reduction and on the other also targets the sub-population of slow cycling label-retaining cells, targeting the more tumorigenic and chemoresistant cells.

According to their ROS production and ALDH1A activity, melanoma tumors are posited as one of the best candidate/s to target ALDH1 within solid tumors. The elevated ALDH1 activity correlated with the mRNA and protein expression amounts of ALDH1A1 and ALDH1A3 isoforms. ALDH1A1 and ALDH1A3 have been suggested as melanoma CSC markers and proteins involved in metastasis.[20,21,38] However, the existence of this cell population enriched in ALDH activity in melanoma is still controversial.[6,39,44] Our results, supported by data analysis from three public databases, show that the *ALDH1A3* isoform is expressed in melanoma cells and not in normal melanocytes, most likely due to epigenetic changes, and whose regulation needs further characterization. This result argues against previous reports suggesting that these proteins are only expressed in a small percentage of cells within melanoma tumors.[20,38] Interestingly, nevi showed ALDH1A3 nuclear expression in differentiated cells that switched to cytoplasmic expression in less differentiated cells within the nevus. Moreover, its cytoplasmic expression increased significantly during progression (superficial spreading melanoma), suggesting its possible role as a biomarker during the establishment of malignancy. The physiological significance of the increased expression and change of localization of ALDH1A3 during melanoma progression is unknown; however, ALDH1A1 and ALDH1A3 have functional roles in melanoma,[20] lung[45] and breast[46,47] cancer cell migration and invasion, through a mechanism that has not been established and requires further investigation.

The correlation between a high amount of ROS and ALDH1 activity in melanoma cells suggests the dependence of these cells on ALDHs for detoxification because of the oxidative processes. In fact, as previously demonstrated *in vitro* in leukemia, prostate and bone marrow cells,[26,27] melanoma cells were sensitive to DIMATE treatment leading to apoptosis, including patient-derived cells. Apoptosis was preceded by the generation of HNE and MDA aldehydes, generating HNE/protein adducts, most likely produced as a consequence of lipid peroxidation induced by ROS.[48] The ability of HNE to form adducts with proteins is the major deleterious event promoted by this molecule.[49] At high concentrations, HNE causes cell cycle arrest,[39,50,51] disturbs differentiation[52,53] and triggers cell death. Importantly, targeting ALDH1A1 and ALDH1A3 with DIMATE reduced *in vivo* tumor growth, including patient-derived xenografts. DIMATE was very well tolerated, promoting systemic alterations only at high concentrations in a daily administration without any obvious therapeutic benefit over a 3 days per week regime. These results are consistent with the bio-distribution of the drug where DIMATE can be detected in liver and kidney 48 h after treatment while it is barely detected in skin, thus, high dose daily treatments may lead to an excessive accumulation of DIMATE in these organs. As normal melanocytes do not express ALDH1A1 and ALDH1A3 isoforms, DIMATE could be mainly acting on tumor cells. Moreover, we did not detect any common side effects in mice described for disulfiram (an ALDH inhibitor), such as skin reactions, drowsiness or unusual tiredness.

In addition, it has been suggested that ALDH1A isoenzymes are markers of melanoma SCs. Depletion of *ALDH1A1* decreased tumorigenicity, tumor growth and metastasis of human melanoma.[20] Our results and the data analysis from three different public databases suggest that between 20 and 60% of the tumors expressed moderate to large amounts of ALDH1A3 and ALDH1A1. This finding does not exclude that the more tumorigenic and/or chemoresistant subset of cells also expresses these proteins. We exploited the slow cycling feature associated with the chemoresistant cell reservoir to confirm that DIMATE was also targeting these cell sub-populations *in vitro* and *in vivo*. DIMATE had an additional therapeutic value by also targeting a subset of cells that could contain the more tumorigenic and chemoresistant cells. In relation to this finding, silencing *ALDH1A1* and *ALDH1A3* reduced the *in vitro* viability, the proliferation in three-dimensional cultures and melanospheres formation promoting apoptosis and markedly reduced cell tumorigenicity, thus validating DIMATE's targets. The synergic effect observed with the simultaneous ablation of both isoforms (*ALDH1A1* and *ALDH1A3)* is consistent with the experimental evidence supporting multi-enzyme isoform participation within the same tumor, where more than one ALDH isoform may be contributing to the progression, exerting some overlapping functions.[54] ALDHs stand out among the expansive group of CSC markers because of their widespread association with different types of solid tumors and the multiplicity of their biological functions, including retinoic acid signaling, antioxidant protection, osmoregulation, drug metabolism and structural support (reviewed in Rodriguez-Torres and Allan[54]). Thus, DIMATE would be acting by inhibiting some or all of these critical processes, most of them exacerbated in both bulk tumor cells and in slow cycling tumor cells.

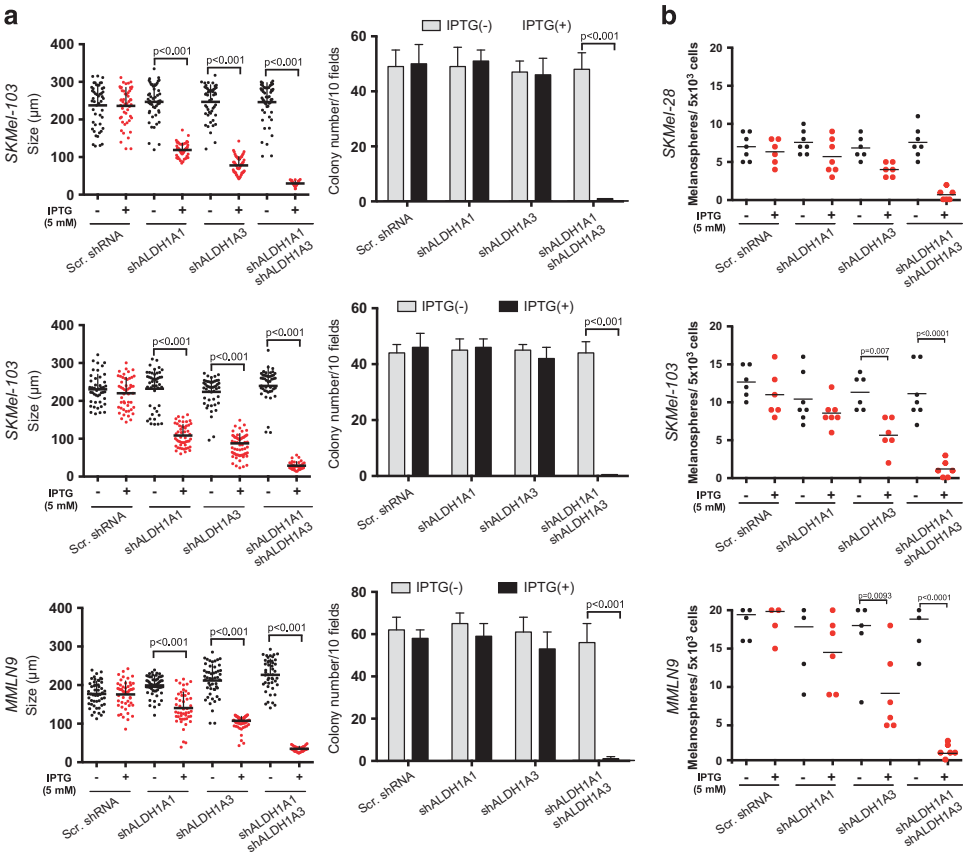

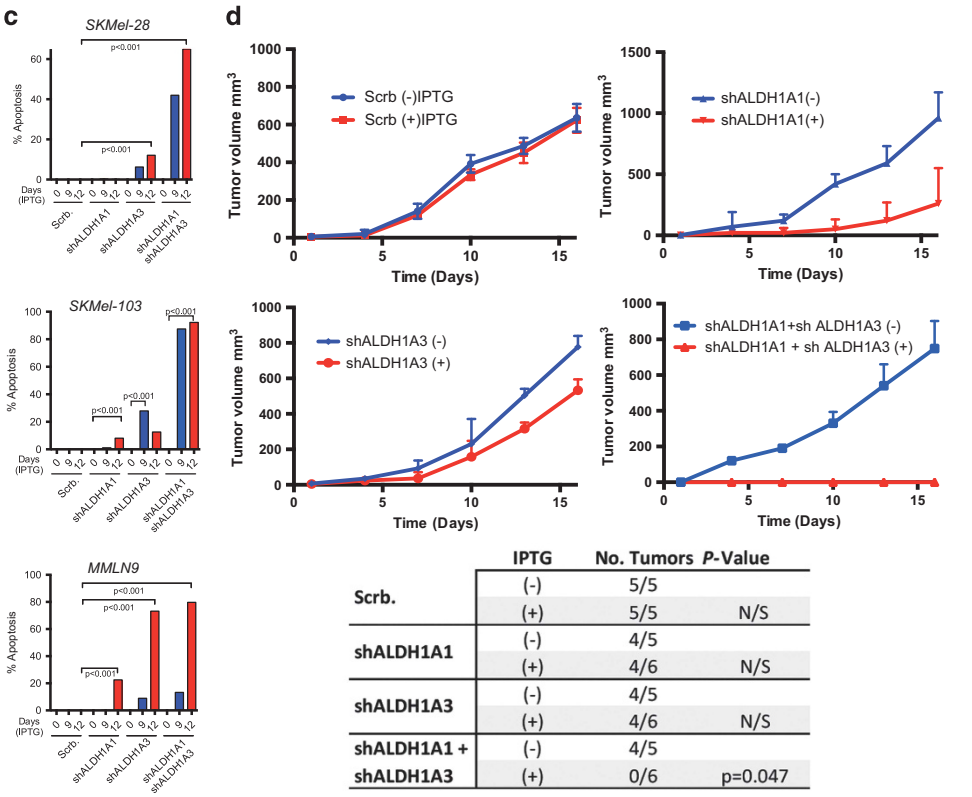

	IPTG	No. Tumors	*P*-Value
Scrb.	(-)	5/5	
	(+)	5/5	N/S
shALDH1A1	(-)	4/5	
	(+)	4/6	N/S
shALDH1A3	(-)	4/5	
	(+)	4/6	N/S
shALDH1A1 + shALDH1A3	(-)	4/5	
	(+)	0/6	p=0.047

The results presented provide evidence supporting the expression of ALDH1A3 as a biomarker of melanocyte evolution to malignancy, which is correlated with the elevated amount of ROS present in melanoma cells, and the detoxification mechanisms that these tumor cells express. Indeed, ALDH1A1 and ALDH1A3 are shown to be critical for the survival and tumorigenicity of melanoma cells. Targeting ALDH1A1 and ALDH1A3 with the novel competitive irreversible inhibitor DIMATE, reduced melanoma tumor growth while simultaneously eliminated slow cycling cells, containing the reservoir of chemoresistant tumor cells. Together, these results offer a novel therapeutic opportunity for melanoma treatment targeting a specific cell metabolic pathway.

MATERIALS AND METHODS

Reagents

The isopropyl β-D-thiogalactoside (IPTG), doxycycline and the Ponceau S solution were obtained from Sigma-Aldrich Quimica (Madrid, Spain). Ficoll Paque was from BD Biosciences (Madrid, Spain). Horseradish linked to peroxidase and fluorescence secondary antibodies were from GE Healthcare (Little Calfont, UK) and Thermo Scientific (Fremont, CA, USA), respectively. Anti-HNE, anti-MDA and Ki67 antibodies were purchased from Abcam (Cambridge, UK). Anti-phospho ERK1/2, anti-cleaved caspase-3, anti-p-S6 and anti-BAX were purchased from Cell Signaling (Leiden, The Netherlands). Anti-ALDH1A1 and anti-hTRA-1-85/CD147 antibodies were from R&D Systems (Minneapolis, MN, USA). Anti-ALDH1A3 was from Abgent (San Diego, CA, USA) and anti-ALDH3A1 was from Sigma-Aldrich. Anti-Bcl-xL was from Biolegend (Fell, Germany), anti-GAPDH was from Trevigen (Gaithersburg, MD, USA), anti-TRP-1 was from Millipore (Temecula, CA, USA), anti-ERK2 was from Santa Cruz Biotechnology (Heidelberg, Germany) and anti-cyclin D1 and anti-Trp-1 were from Thermo Scientific. Sorafenib, salirasib, cisplatin, carboplatin, dacarbazine and paclitaxel were purchased from Sellekchem (Deltaclon, S.L, Madrid, Spain). 4-Dimethylamino-4-methyl-pent-2-ynthioic acid-S methylester (DIMATE) was provided by Advanced BioDesign (Saint Priest, France).

Cancer cell lines

Melanoma samples from patients were collected during surgical operations with the informed consent of the patients and the Vall d´Hebron Hospital ethical committee approval PR(AG)59/2009. Tumor samples, including both primary and metastatic lesions (18 different samples 7 paired tumors from same patient), and 23 nevi were obtained as paraffin-embedded material.

For patient-derived melanoma cells (MMPG3, MMLN8, MMLN9, MMLN10 and MmBr12), tumors were disaggregated by mechanical and enzymatic disruption[55] and cultured in Melanocyte Growth Medium M2 (PromoCell GmbH, Heidelberg Germany) supplemented with antibiotics. Normal human epidermal melanocytes were obtained from PromoCell (Heidelberg, Germany) and were cultured in melanocyte growth medium M2 (PromoCell). 37-31E mouse melanoma cells were described previously.[56,57] MMLN9 patient-derived cells were infected immediately after tumor disaggregation either with the doxycycline inducible construct rtTA2-H2B-GFP (containing the fusion protein Histone 2B (H2B-GFP)) or rtTA2-GFP expression vectors (generated by S Tenbaum, HG Palmer's Lab, VHIO, Barcelona, Spain).

Xenograft-derived cancer cells of breast, ovary and colon tumors were provided by Advanced BioDesign. UACC-903 cells were a gift from J Trent (P Pollock, Tgen, Phoenix, AZ, USA). SkMel-147 and SKMel-103 cells were obtained from M Soengas (CNIO Madrid, Spain). H1650, H1975, HCC2935, HCC4006, H1299, Hop62, H820 and H23 were generously gifted to us by Dr Yokota (Institute of predictive and personalized Medicine of Cancer, Barcelona, Spain). LNCap, PC3, DU145, MIA PaCa-2, SK-OV-3, OVCAR-3 and OVCAR-4 were obtained from R Paciucci and A Santamaria (VHIR, Barcelona, Spain). MeWo, SKMel-28, A375, G361, HCC827, H441, A549, H522, MCF-7, MDA-MB-231, MDA-MB-468, U-87, HL-60, Kasumi-1 and THP-1 cells were purchased from the American Type Culture Collection (ATCC, Manassas, VA, USA). UACC-903, LNCap, PC3, OVCAR-3, OVCAR-4, H1650, H1975, HCC2935, HCC4006, H1299, Hop62, H820, H23, HCC827, H441, H522, HL-60, Kasumi-1 and THP-1 cells were cultured in RPMI. MIA PaCa-2, A549, SKMel-103, SkMel-147, A375, G361, MCF-7, MDA-MB-231 and MDA-MB-468 were maintained in Dulbecco's modified Eagle's medium. DU145, SKMel-28, MeWo and U-87 were cultured in Eagle's minimal essential medium and SK-OV-3 was cultured in McCoy's 5 A medium. All of the media were supplemented with 10% fetal bovine serum, 2 mM L-glutamine, 100 IU/ml penicillin and 100 μg/ml streptomycin. Cells were grown at 37 °C and 5% CO_2 conditions and tested for mycoplasma contamination.

Immunoblots

Cells were lysed in RIPA lysis buffer, equal amounts of protein were subjected to sodium dodecyl sulfate–polyacrylamide gel electrophoresis and transferred to a polyvinylidene difluoride membrane. Immunoblots were performed as previously described.[56,57]

Detection of total ROS and ALDH1 activity

Cellular ROS production was measured using the total ROS/superoxide detection kit (Enzo Life Science, Lausen, Switzerland), following the manufacturer's instructions. ALDH1 activity assay was performed using the fluorescence probe GFSEF12 (Advanced BioDesign, patent application:1657324) (ALDH1: $Vmax/K_m = 105.04$; ALDH2: $Vmax/K_m = 37.69$; ALDH3: $Vmax/K_m = 18.29$). Cells were seeded into 96-well plates. For ALDH1 activity, cells were incubated with GFSEF12 (1.6 μM) for 60 min at 37 °C. Fluorescence was detected using an Appliskan fluorescence microplate reader (Thermo Scientific) (ex = 530–560 nm, Em = 590–600 nm). DIMATE was used as control for the specific interaction of GFSEF12 with the ALDH1 isoenzymes. For the evaluation of the drug effect in the presence of a ROS scavenger, 1×10^5 cells were plated in six-well plates and pre-treated with *N*-acetyl-cysteine (5 mM) (Sigma-Aldrich) or with the reduced glutathione-monoethyl-ester analog for 30 min before addition of DIMATE. After the indicated times (6, 12 and 24 h), cell viability was calculated using Trypan blue exclusion dye (0.1%, Sigma-Aldrich) and a hemocytometer (Marienfeld, Germany). The results are expressed as percentage (%) of cell death.

Quantitative reverse transcriptase–PCR

Total RNA extraction was performed using TRIzol (Thermo Scientific) following the manufacturer's instructions. Complementary DNA was generated using the Superscript III first-strand synthesis SuperMix (Thermo Fisher). Quantitative PCR analysis was performed using the SYBR Green PCR Master Mix Kit (Applied Biosystems Inc., Foster City, CA, USA) and the ABI Prism 7900HT Fast Real-Time PCR System (Applied Biosystems Inc.). Primer sequences for the different ALDHs isoforms are shown in the Supplementary Figure S3. h*VIM*, h*ACTB* and h*SF3A1* genes were used for normalization.

DNA methylation detection

GDNA was obtained from human cells. Genomic DNA was fragmented into 300–500-bp fragments using a Covaris ultra-sonicator (Covaris, Woburn,

Figure 6. Depletion of *ALDH1A1* and *ALDH1A3* impedes *in vitro* and *in vivo* tumor growth and viability, promoting apoptosis. (**a**) Three-dimensional colony formation assay using SKMel-28, SKMel-103 and MMLN9 patient-derived cells stably transduced with an IPTG-inducible expression system for either shALDH1A or shALDH1A3 or both. Graphs show the size of the colonies and the colony number for each condition ($n = 50$ colonies per condition). *P*-value was calculated by *t*-test. The experiments were performed in triplicate. (**b**) Melanospheres formation assay using same cells as in **a**. Graphs show the number of melanospheres formed in six independent experiments (dots) under the different conditions. *P*-value was calculated by *t*-test. (**c**) Depletion of ALDH1A1 and/or ALDH1A3 induces apoptosis. Percentage of apoptotic cells at 9 and 12 days after IPTG (5 mM) treatment measured by PI: propidium iodide, Annexin V: GFP-annexin V staining. A representative experiment out of three is shown. *P*-value was calculated by Student's *t*-test. (**d**) *In vivo* tumor growth of SKMel-103 cells stably transduced with an IPTG-inducible expression system for either shALDH1A or shALDH1A3 or both. Table shows the number mice developing tumors in each group. *P*-value was calculated by a two-tailed binomial test.

MA, USA). Fragmented DNA was then subjected to methylation analysis using a MethylCap kit (Diagenode, Liège, Belgium) according to the manufacturer's recommended protocol. SYBR green real-time PCR (Applied Biosystems) was performed using two sets of primers for the *ALDH1A3* promoter CpG islands (see table in Supplementary Figure S3C) to quantify the specific isolated methylated DNA. The manufacturer provided the primers for CpG islands of *TSH2B*, which was used as a positive control for methylation, and primers for *GAPDH*, which was used as a control for non-methylation. Melting curves were analyzed to confirm methylation-specific PCR products.

Cytotoxicity assays

Cells were seeded into 96-well cell culture plates. The growth-inhibitory effect of the drugs was analyzed using an *in vitro*, Resazurin based toxicity assay, following the manufacturer's instructions (Sigma-Aldrich). The drug response was quantified by the half maximal inhibitory concentration (IC_{50}) and determined by non-linear regression analysis of log-dose/response curves. The cut-off value to define cell resistance to DIMATE was determined statistically (above IC_{50} geometric mean+s.d.). The *in vitro* threshold value for high sensitivity to DIMATE was defined as $< IC_{50}$ geometric mean. All of the time points were performed in triplicate.

Apoptosis assays

Cells were stained with either annexin V–GFP or annexin V-allophycocyanin together with propidium iodide and evaluated for apoptosis by flow cytometry according to the manufacturer's protocol (Biovision, Milpitas, CA, USA).

Small interfering RNA and shRNA assays

For transient experiments, cells were transfected with either a scrambled small interfering RNA or three different small interfering RNAs targeting *ALDH1A1* or *ALDH1A3* from Invitrogen-Thermo Scientific (see Supplementary Figure S8A for sequences). For the inducible system, cells were infected with hu-ALDH1A1 and/or hu-ALDH1A3 Mission-custom shRNA lentiviral particles (pLKO-puro-3xLacO-shALDH1A1, pLKO-puro-3xLacO-shALDH1A3) (Sigma-Aldrich) (sequences of shRNAs are depicted in Supplementary Figure S7A). The control vector used was a pLKO backbone based IPTG-inducible non-targeting shRNA (pLKO-puro-IPTG--3xLacO-shNT (SHC332V; Sigma-Aldrich). For shRNA expression, culture medium was supplemented with 5 mM IPTG, routinely, for 7 days. Knockdown efficiency was evaluated by quantitative reverse transcriptase–PCR and western blot analysis.

Soft agar clonogenicity assay and melanospheres formation assay

For clonogenicity assays, 10 000 cells were seeded into 0.4% low melting point agarose (Lonza, Barcelona, Spain) on top of a 1% agarose layer. The cells were incubated in complete supplemented media, in the presence or absence of IPTG (1 mM), under growth conditions, for 3 weeks. Colonies were observed under an inverted microscope (NIKON eclipse TE2000-S, Amsterdam, The Netherlands) at ×4 magnification. Ten microscopic fields were randomly chosen from each well and the data were shown as the mean ± s.e. from three independent experiments. For melanospheres formation, 5×10^3 single cells were plated in ultralow-attachment plates (Corning, Madrid, Spain) in PromoCell CSC medium, following the manufacturer's protocol (PromoCell GmgH, Heidelberg, Germany). Cells were maintained at 37 °C in a humidified atmosphere containing 5% CO_2. Every second day fresh media, with or without IPTG (5 mM), were added into the cell cultures. Cells were grown under these conditions for 21 days and subsequently, spheres were counted and photographed.

Immunohistochemistry and immunofluorescence

Formalin-fixed paraffin-embedded tumor samples were subjected to immunocytochemistry according to the manufacturer's antibody protocol. Samples were developed either by using secondary antibodies linked to horseradish peroxidase or secondary antibodies linked to a fluorophore. Immunostaining was performed on 4 μm sections from formalin-fixed paraffin-embedded tissues. Staining was performed either manually or on an automated immunostainer Beckmarck XT (Ventana Medical Systems, Tucson, AZ, USA). Antibodies were visualized by the UltraView Universal DAB detection Kit (Ventana Medical Systems). Samples were evaluated by two independent pathologists.

Animal experiments

All of the mice were cared for and maintained in accordance with animal welfare regulations under an approved protocol by the Institutional Animal Care and Use Committee of Vall d'Hebron Research Institute (VHIR). For xenograft animal models, 5×10^5 human SKMel-103, SKMel-28 or MMLN9-H2B-GFP cells were subcutaneously implanted in 8-week-old females athymic Nude-*Foxn1nu* mice ($n = 5$ per group) (Envigo, Indianapolis, IN, USA). For the syngeneic model, tumors were generated as previously described.[56,57] When the tumors reached a volume between 50 and 100 mm^3, mice with similarly sized tumors were randomized into treatment cohorts ($n = 6$ per group). Treated groups received an i.p. injection of DIMATE (14, 28 or 42 mg/kg) once every third day for 3–4 weeks or daily. Control groups were treated with vehicle (Hepes 10 mM).

Mice bearing MMLN9-H2B-GFP tumor xenografts received doxycycline to regulate the expression of H2B-GFP. Mice received either (1) normal drinking water, (2) drinking water with 0.2 mg/ml doxycycline, (3) drinking water with 0.2 mg/ml doxycycline as in '2' except that doxycycline was withdrawn at the starting time of treatment (when tumors were 50–100 mm^3) or (4) and (5) drinking water with 0.2 mg/ml doxycycline (same schedule as in '3') in combination with i.p. injection of 7 mg/kg or 14 mg/kg of DIMATE, respectively.

For *in vivo* inducible shRNA expression, one million MMLN9 cells infected with lentiviral particles (pLKO-puro-3xLacO-shALDH1A1, pLKO-puro-3xLacOsh-ALDH1A3, and pLKO-puro-IPTG-3xLacO-shNT) were implanted subcutaneously. Mice received 20 mM IPTG in drinking water (bottles were changed three times per week). Tumors were measured with a digital Vernier caliper, and the mice weighed twice a week. Tumor volume was calculated with the following equation: tumor volume (mm^3) = (length × width × height)/2. The results are presented as tumor volume mean ± s.e.

Blood tests

Blood from animals were obtained at the end point of the experiments. Blood samples were always collected during the same time interval in the afternoon (1500 to 1530 hours) after a fasting period of 5 h. For hematology, blood was collected in microtubes containing EDTA. The tests were performed on a Hemavet 950FS Multi Species Hematology System (Drew Scientific, Waterbury, CT, USA) programmed with mouse hematology settings. Sample processing and system maintenance were performed as described in the manufacturer's operating instructions. For enzymatic measures, the samples were analyzed using a chemistry analyzer (SPOTCHEM EZ, Arkray Factory, Inc., AT Amstelveen, The Netherlands) using dry chemistry technology. Kidney and hepatic enzymatic panels were used for each sample following the manufacturer´s recommendations.

Isolation of MMLN9-H2B-GFP cells from tumor xenografts and FACS analyses

Tumors were excised, minced into < 1 mm pieces, and enzymatically dissociated. Cell suspensions were passed through a 100 μm cell strainer (BD Biosciences, Franklin Lakes, NJ, USA), and single cells were collected by centrifugation at 400 *g* for 5 min. To remove red blood cells and cellular debris, cells were incubated for 10 min with RBC lysis buffer (eBioscience, San Diego, CA, USA), washed with Dulbecco's modified Eagle's medium and layered on 7.5 ml Ficoll Paque. Following centrifugation at 400 *g* for 25 min, the cells were collected from the interphase and washed with phosphate-buffered saline.

For flow cytometry analysis, the cells were incubated with an allophycocyanin-labeled CD147 antibody for 1 h at 4 °C. Following staining, the cells were washed and resuspended in fluorescence-activated cell sorting (FACS) buffer. Propidium iodide was added to the final solution to distinguish live/dead cells. The quantification of human GFP-positive cells was performed on a FACS-Fortessa (BD Biosciences, San Jose, CA, USA). To eliminate the mouse cell population, CD147-negative cells were excluded from the analysis.

Statistical analyses

ImageJ software (NIH, Bethesda, MD, USA) was used for the quantification of the signal, and GraphPad Prism (GraphPad Software, Inc., La Jolla, CA, USA) v6.0d was used for the graphic representation and statistical analysis of the data. The significance of the differences between groups in mouse

experiments was determined using analysis of variance analysis in GraphPad Prism v6.0d. Tukey's test was used in the post analysis, and the differences were considered significant if the *P*-value was $\leqslant 0.05$. Comparisons between groups were performed with Student's *t*-test using GraphPad Prism v6.0d. All of the statistical analyses were two-sided, and *P*-values $\leqslant 0.05$ were considered significant.

CONFLICT OF INTEREST

The authors declare no conflict of interest.

ACKNOWLEDGEMENTS

Dr G Quash is gratefully acknowledged for critical reading of the manuscript and his contributions. We also thank Dr HG Palmer for his generous contribution. This work was supported by funds from Advanced BioDesign (MPA), the Spanish Health Ministry (Fondo de Investigaciones Sanitarias-FIS) PI1400375-Fondos FEDER, AECC-GCB15152978SOEN, Marie Curie Actions (IEF_METABOSET-627869) supported MPA.

REFERENCES

1 Miller KD, Siegel RL, Lin CC, Mariotto AB, Kramer JL, Rowland JH *et al.* Cancer treatment and survivorship statistics, 2016. *CA Cancer J Clin* 2016; **66**: 271–289.
2 Delyon J, Mateus C, Lefeuvre D, Lanoy E, Zitvogel L, Chaput N *et al.* Experience in daily practice with ipilimumab for the treatment of patients with metastatic melanoma: an early increase in lymphocyte and eosinophil counts is associated with improved survival. *Ann Oncol* 2013; **24**: 1697–1703.
3 Hodi FS, O'Day SJ, McDermott DF, Weber RW, Sosman JA, Haanen JB *et al.* Improved survival with ipilimumab in patients with metastatic melanoma. *N Engl J Med* 2010; **363**: 711–723.
4 Sosman JA, Kim KB, Schuchter L, Gonzalez R, Pavlick AC, Weber JS *et al.* Survival in BRAF V600-mutant advanced melanoma treated with vemurafenib. *N Engl J Med* 2012; **366**: 707–714.
5 Vasiliou V, Pappa A, Petersen DR. Role of aldehyde dehydrogenases in endogenous and xenobiotic metabolism. *Chem Biol Interact* 2000; **129**: 1–19.
6 Vasiliou V, Nebert DW. Analysis and update of the human aldehyde dehydrogenase (ALDH) gene family. *Hum Genomics* 2005; **2**: 138–143.
7 Yoshida A, Hsu LC, Dave V. Retinal oxidation activity and biological role of human cytosolic aldehyde dehydrogenase. *Enzyme* 1992; **46**: 239–244.
8 Blackwell LF, Bennett AF, Buckley PD. Relationship between the mechanisms of the esterase and dehydrogenase activities of the cytoplasmic aldehyde dehydrogenase from sheep liver. An alternative view. *Biochemistry* 1983; **22**: 3784–3791.
9 Chen Y, Mehta G, Vasiliou V. Antioxidant defenses in the ocular surface. *Ocul Surf* 2009; **7**: 176–185.
10 Estey T, Cantore M, Weston PA, Carpenter JF, Petrash JM, Vasiliou V. Mechanisms involved in the protection of UV-induced protein inactivation by the corneal crystallin ALDH3A1. *J Biol Chem* 2007; **282**: 4382–4392.
11 Marchitti SA, Brocker C, Stagos D, Vasiliou V. Non-P450 aldehyde oxidizing enzymes: the aldehyde dehydrogenase superfamily. *Expert Opin Drug Metab Toxicol* 2008; **4**: 697–720.
12 Marcato P, Dean CA, Giacomantonio CA, Lee PW. Aldehyde dehydrogenase: its role as a cancer stem cell marker comes down to the specific isoform. *Cell Cycle* 2011; **10**: 1378–1384.
13 Cheung AM, Wan TS, Leung JC, Chan LY, Huang H, Kwong YL *et al.* Aldehyde dehydrogenase activity in leukemic blasts defines a subgroup of acute myeloid leukemia with adverse prognosis and superior NOD/SCID engrafting potential. *Leukemia* 2007; **21**: 1423–1430.
14 Charafe-Jauffret E, Ginestier C, Bertucci F, Cabaud O, Wicinski J, Finetti P *et al.* ALDH1-positive cancer stem cells predict engraftment of primary breast tumors and are governed by a common stem cell program. *Cancer Res* 2013; **73**: 7290–7300.
15 Dylla SJ, Beviglia L, Park IK, Chartier C, Raval J, Ngan L *et al.* Colorectal cancer stem cells are enriched in xenogeneic tumors following chemotherapy. *PLoS One* 2008; **3**: e2428.
16 Huang EH, Hynes MJ, Zhang T, Ginestier C, Dontu G, Appelman H *et al.* Aldehyde dehydrogenase 1 is a marker for normal and malignant human colonic stem cells (SC) and tracks SC overpopulation during colon tumorigenesis. *Cancer Res* 2009; **69**: 3382–3389.
17 Ma S, Chan KW, Lee TK, Tang KH, Wo JY, Zheng BJ *et al.* Aldehyde dehydrogenase discriminates the CD133 liver cancer stem cell populations. *Mol Cancer Res* 2008; **6**: 1146–1153.
18 Rasheed ZA, Yang J, Wang Q, Kowalski J, Freed I, Murter C *et al.* Prognostic significance of tumorigenic cells with mesenchymal features in pancreatic adenocarcinoma. *J Natl Cancer Inst* 2010; **102**: 340–351.
19 van den Hoogen C, van der Horst G, Cheung H, Buijs JT, Lippitt JM, Guzman-Ramirez N *et al.* High aldehyde dehydrogenase activity identifies tumor-initiating and metastasis-initiating cells in human prostate cancer. *Cancer Res* 2010; **70**: 5163–5173.
20 Luo Y, Dallaglio K, Chen Y, Robinson WA, Robinson SE, McCarter MD *et al.* ALDH1A isozymes are markers of human melanoma stem cells and potential therapeutic targets. *Stem Cells* 2012; **30**: 2100–2113.
21 Yue L, Huang ZM, Fong S, Leong S, Jakowatz JG, Charruyer-Reinwald A *et al.* Targeting ALDH1 to decrease tumorigenicity, growth and metastasis of human melanoma. *Melanoma Res* 2015; **25**: 138–148.
22 Januchowski R, Wojtowicz K, Zabel M. The role of aldehyde dehydrogenase (ALDH) in cancer drug resistance. *Biomed Pharmacother* 2013; **67**: 669–680.
23 Alnouti Y, Klaassen CD. Tissue distribution, ontogeny, and regulation of aldehyde dehydrogenase (Aldh) enzymes mRNA by prototypical microsomal enzyme inducers in mice. *Toxicol Sci* 2008; **101**: 51–64.
24 Koppaka V, Thompson DC, Chen Y, Ellermann M, Nicolaou KC, Juvonen RO *et al.* Aldehyde dehydrogenase inhibitors: a comprehensive review of the pharmacology, mechanism of action, substrate specificity, and clinical application. *Pharmacol Rev* 2012; **64**: 520–539.
25 Roch AM, Quash G, Michal Y, Chantepie J, Chantegrel B, Deshayes C *et al.* Altered methional homoeostasis is associated with decreased apoptosis in BAF3 bcl2 murine lymphoid cells. *Biochem J* 1996; **313**(Pt 3): 973–981.
26 Quash G, Fournet G, Chantepie J, Gore J, Ardiet C, Ardail D *et al.* Novel competitive irreversible inhibitors of aldehyde dehydrogenase (ALDH1): restoration of chemosensitivity of L1210 cells overexpressing ALDH1 and induction of apoptosis in BAF(3) cells overexpressing bcl(2). *Biochem Pharmacol* 2002; **64**: 1279–1292.
27 Quash G, Fournet G, Courvoisier C, Martinez RM, Chantepie J, Paret MJ *et al.* Aldehyde dehydrogenase inhibitors: alpha,beta-acetylenic N-substituted aminothiolesters are reversible growth inhibitors of normal epithelial but irreversible apoptogens for cancer epithelial cells from human prostate in culture. *Eur J Med Chem* 2008; **43**: 906–916.
28 Monneuse O, Mestrallet JP, Quash G, Gilly FN, Glehen O. Intraperitoneal treatment with dimethylthioampal (DIMATE) combined with surgical debulking is effective for experimental peritoneal carcinomatosis in a rat model. *J Gastrointest Surg* 2005; **9**: 769–774.
29 Wittgen HG, van Kempen LC. Reactive oxygen species in melanoma and its therapeutic implications. *Melanoma Res* 2007; **17**: 400–409.
30 Esterbauer H, Eckl P, Ortner A. Possible mutagens derived from lipids and lipid precursors. *Mutat Res* 1990; **238**: 223–233.
31 Summerfield FW, Tappel AL. Cross-linking of DNA in liver and testes of rats fed 1,3-propanediol. *Chem Biol Interact* 1984; **50**: 87–96.
32 Townsend AJ, Leone-Kabler S, Haynes RL, Wu Y, Szweda L, Bunting KD. Selective protection by stably transfected human ALDH3A1 (but not human ALDH1A1) against toxicity of aliphatic aldehydes in V79 cells. *Chem Biol Interact* 2001; **130-132**: 261–273.
33 Hill BG, Bhatnagar A. Beyond reactive oxygen species: aldehydes as arbitrators of alarm and adaptation. *Circ Res* 2009; **105**: 1044–1046.
34 Grammatico P, Maresca V, Roccella F, Roccella M, Biondo L, Catricala C *et al.* Increased sensitivity to peroxidizing agents is correlated with an imbalance of antioxidants in normal melanocytes from melanoma patients. *Exp Dermatol* 1998; **7**: 205–212.
35 Jackson B, Brocker C, Thompson DC, Black W, Vasiliou K, Nebert DW *et al.* Update on the aldehyde dehydrogenase gene (ALDH) superfamily. *Hum Genomics* 2011; **5**: 283–303.
36 Venza M, Visalli M, Beninati C, De Gaetano GV, Teti D, Venza I. Cellular mechanisms of oxidative stress and action in melanoma. *Oxid Med Cell Longev* 2015; **2015**: 481782.
37 Tomita H, Tanaka K, Tanaka T, Hara A. Aldehyde dehydrogenase 1A1 in stem cells and cancer. *Oncotarget* 2016; **7**: 11018–11032.
38 Boonyaratanakornkit JB, Yue L, Strachan LR, Scalapino KJ, LeBoit PE, Lu Y *et al.* Selection of tumorigenic melanoma cells using ALDH. *J Invest Dermatol* 2010; **130**: 2799–2808.
39 Prasmickaite L, Engesaeter BO, Skrbo N, Hellenes T, Kristian A, Oliver NK *et al.* Aldehyde dehydrogenase (ALDH) activity does not select for cells with enhanced aggressive properties in malignant melanoma. *PLoS ONE* 2010; **5**: e10731.
40 Burger PE, Gupta R, Xiong X, Ontiveros CS, Salm SN, Moscatelli D *et al.* High aldehyde dehydrogenase activity: a novel functional marker of murine prostate stem/progenitor cells. *Stem Cells* 2009; **27**: 2220–2228.

41 Fournet G, Martin G, Quash G. alpha,beta-Acetylenic amino thiolester inhibitors of aldehyde dehydrogenases 1&3: suppressors of apoptogenic aldehyde oxidation and activators of apoptosis. *Curr Med Chem* 2013; **20**: 527–533.
42 Moore N, Lyle S. Quiescent, slow-cycling stem cell populations in cancer: a review of the evidence and discussion of significance. *J Oncol* 2011; **2011**: 1–11.
43 Moore N, Houghton J, Lyle S. Slow-cycling therapy-resistant cancer cells. *Stem Cells Dev* 2012; **21**: 1822–1830.
44 Quintana E, Shackleton M, Sabel MS, Fullen DR, Johnson TM, Morrison SJ. Efficient tumour formation by single human melanoma cells. *Nature* 2008; **456**: 593–598.
45 Li X, Wan L, Geng J, Wu CL, Bai X. Aldehyde dehydrogenase 1A1 possesses stem-like properties and predicts lung cancer patient outcome. *J Thorac Oncol* 2012; **7**: 1235–1245.
46 Marcato P, Dean CA, Liu RZ, Coyle KM, Bydoun M, Wallace M *et al*. Aldehyde dehydrogenase 1A3 influences breast cancer progression via differential retinoic acid signaling. *Mol Oncol* 2015; **9**: 17–31.
47 Moreb JS, Baker HV, Chang LJ, Amaya M, Lopez MC, Ostmark B *et al*. ALDH isozymes downregulation affects cell growth, cell motility and gene expression in lung cancer cells. *Mol Cancer* 2008; **7**: 87.
48 Dalleau S, Baradat M, Gueraud F, Huc L. Cell death and diseases related to oxidative stress: 4-hydroxynonenal (HNE) in the balance. *Cell Death Differ* 2013; **20**: 1615–1630.
49 Sovic A, Borovic S, Loncaric I, Kreuzer T, Zarkovic K, Vukovic T *et al*. The carcinostatic and proapoptotic potential of 4-hydroxynonenal in HeLa cells is associated with its conjugation to cellular proteins. *Anticancer Res* 2001; **21**: 1997–2004.
50 Pizzimenti S, Barrera G, Dianzani MU, Brusselbach S. Inhibition of D1, D2, and A-cyclin expression in HL-60 cells by the lipid peroxydation product 4-hydroxynonenal. *Free Radic Biol Med* 1999; **26**: 1578–1586.
51 Wonisch W, Kohlwein SD, Schaur J, Tatzber F, Guttenberger H, Zarkovic N *et al*. Treatment of the budding yeast Saccharomyces cerevisiae with the lipid peroxidation product 4-HNE provokes a temporary cell cycle arrest in G1 phase. *Free Radic Biol Med* 1998; **25**: 682–687.
52 Barrera G, Di Mauro C, Muraca R, Ferrero D, Cavalli G, Fazio VM *et al*. Induction of differentiation in human HL-60 cells by 4-hydroxynonenal, a product of lipid peroxidation. *Exp Cell Res* 1991; **197**: 148–152.
53 Pizzimenti S, Laurora S, Briatore F, Ferretti C, Dianzani MU, Barrera G. Synergistic effect of 4-hydroxynonenal and PPAR ligands in controlling human leukemic cell growth and differentiation. *Free Radic Biol Med* 2002; **32**: 233–245.
54 Rodriguez-Torres M, Allan AL. Aldehyde dehydrogenase as a marker and functional mediator of metastasis in solid tumors. *Clin Exp Metastasis* 2016; **33**: 97–113.
55 Tenbaum SP, Ordonez-Moran P, Puig I, Chicote I, Arques O, Landolfi S *et al*. Beta-catenin confers resistance to PI3K and AKT inhibitors and subverts FOXO3a to promote metastasis in colon cancer. *Nat Med* 2012; **18**: 892–901.
56 Andreu-Perez P, Hernandez-Losa J, Moline T, Gil R, Grueso J, Pujol A *et al*. Methylthioadenosine (MTA) inhibits melanoma cell proliferation and *in vivo* tumor growth. *BMC Cancer* 2010; **10**: 265.
57 Lopez-Fauqued M, Gil R, Grueso J, Hernandez-Losa J, Pujol A, Moline T *et al*. The dual PI3K/mTOR inhibitor PI-103 promotes immunosuppression, in vivo tumor growth and increases survival of sorafenib-treated melanoma cells. *Int J Cancer* 2010; **126**: 1549–1561.

Supplementary Information accompanies this paper on the Oncogene website (http://www.nature.com/onc)